

Incorporation of an Amide into 5-Phosphonoalkyl-6-D-ribitylamino-2,4-pyrimidinedione Lumazine Synthase Inhibitors Results in an Unexpected Reversal of Selectivity for Riboflavin Synthase vs Lumazine Synthase

Mark Cushman,^{*,†} Donglai Yang,[†] Jeffrey T. Mihalic,[†] Jinhua Chen,[†] Stefan Gerhardt,^{‡,§}
Robert Huber,[§] Markus Fischer,[‡] Klaus Kis,[‡] and Adelbert Bacher[‡]

Department of Medicinal Chemistry and Molecular Pharmacology, School of Pharmacy and Pharmacal Sciences, Purdue University, West Lafayette, Indiana 47907, Lehrstuhl für Organische Chemie und Biochemie, Technische Universität München, D-85747 Garching, Germany, and Max-Planck-Institut für Biochemie, Abteilung Strukturforschung, Am Klopferspitz 18a, D-82152 Martinsried, Germany

cushman@pharmacy.purdue.edu

Received March 1, 2002

Several analogues of a hypothetical intermediate in the reaction catalyzed by lumazine synthase were synthesized and tested as inhibitors of both *Bacillus subtilis* lumazine synthase and *Escherichia coli* riboflavin synthase. The new compounds were designed by replacement of a two-carbon fragment of several 5-phosphonoalkyl-6-D-ribitylamino-2,4-pyrimidinedione lumazine synthase inhibitors with an amide linkage that was envisioned as an analogue of a Schiff base moiety of a hypothetical intermediate in the enzyme-catalyzed reaction. The incorporation of the amide group led to an unexpected reversal in selectivity for inhibition of lumazine synthase vs riboflavin synthase. Whereas the parent 5-phosphonoalkyl-6-D-ribitylamino-2,4-pyrimidinediones were lumazine synthase inhibitors and did not inhibit riboflavin synthase, the amide-containing derivatives inhibited riboflavin synthase and were only very weak or inactive as lumazine synthase inhibitors. Molecular modeling of inhibitor–lumazine synthase complexes did not reveal a structural basis for these unexpected findings. However, molecular modeling of one of the inhibitors with *E. coli* riboflavin synthase demonstrated that the active site of the enzyme could readily accommodate two ligand molecules.

Introduction

Lumazine synthase catalyzes the condensation of 5-amino-6-D-ribitylamino-2,4(1*H*,3*H*)-pyrimidinedione (**1**) with 3,4-dihydroxybutanone 4-phosphate (**2**) to afford 6,7-dimethyl-8-D-ribityllumazine (**3**). Riboflavin synthase then catalyzes the transfer of a four-carbon unit from one molecule of **3** to another molecule of **3** to afford riboflavin (**4**) and **1**, which can be recycled by lumazine synthase (Scheme 1).^{1–5} Since a variety of Gram-negative bacteria and yeasts lack an efficient riboflavin uptake system, the enzymes responsible for riboflavin biosynthesis are rational targets for antibiotic drug development.^{6–13}

The mechanism of the lumazine synthase-catalyzed reaction is thought to proceed as outlined in Scheme 2. Schiff base formation between the two substrates **1** and **2** results in the formation of the imine **5**, which then eliminates phosphoric acid to yield the enol **6**. Tautomerization of the enol **6** to the ketone **7**, followed by a nucleophilic attack by the secondary amino group on the ketone, affords the covalently hydrated lumazine **8**. Loss of a water molecule then yields the final product **3**. The enzyme-bound conformation of the phosphate-containing side chain of the Schiff base intermediate is thought to be close to that shown in structure **5**. The evidence for this includes the X-ray structure of 5-nitro-6-D-ribityl-

[†] Purdue University.

[‡] Technische Universität München.

[§] Max-Planck-Institut.

(1) Plaut, G. W. E.; Smith, C. M.; Alworth, W. L. *Annu. Rev. Biochem.* **1974**, *43*, 899–922.

(2) Plaut, G. W. E. In *Comprehensive Biochemistry*; Florjkin, M., Stotz, E. H., Eds.; Elsevier: Amsterdam, 1971; Vol. 21, pp 11–45.

(3) Beach, R. L.; Plaut, G. W. E. *J. Am. Chem. Soc.* **1970**, *92*, 2913–2916.

(4) Bacher, A.; Eberhardt, S.; Richter, G. In *Escherichia coli and Salmonella: Cellular and Molecular Biology*, 2nd ed.; Neidhardt, F. C., Ed.; ASM Press: Washington, DC, 1996; pp 657–664.

(5) Bacher, A.; Fischer, M.; Kis, K.; Kugelbrey, K.; Mörtl, S.; Scheuring, J.; Weinkauff, S.; Eberhardt, S.; Schmidt-Bäse, K.; Huber, R.; Ritsert, K.; Cushman, M.; Ladenstein, R. *Biochem. Soc. Trans.* **1996**, *24*, 89–94.

(6) Bandrin, S. V.; Beburow, M. Y.; Rabinovich, P. M.; Stepanov, A. I. *Genetika* **1979**, *15*, 2063–2065.

(7) Shavlovskii, G. M.; Teslyar, G. E.; Strugovshchikova, L. P. *Mikrobiologiya* **1982**, *1979*, 986–992.

(8) Oltmanns, O.; Lingens, F. *Z. Naturforschung.* **1967**, *22*, 751–754.

(9) Logvinenko, E. M.; Shavlovsky, G. M. *Mikrobiologiya* **1967**, *41*, 978–979.

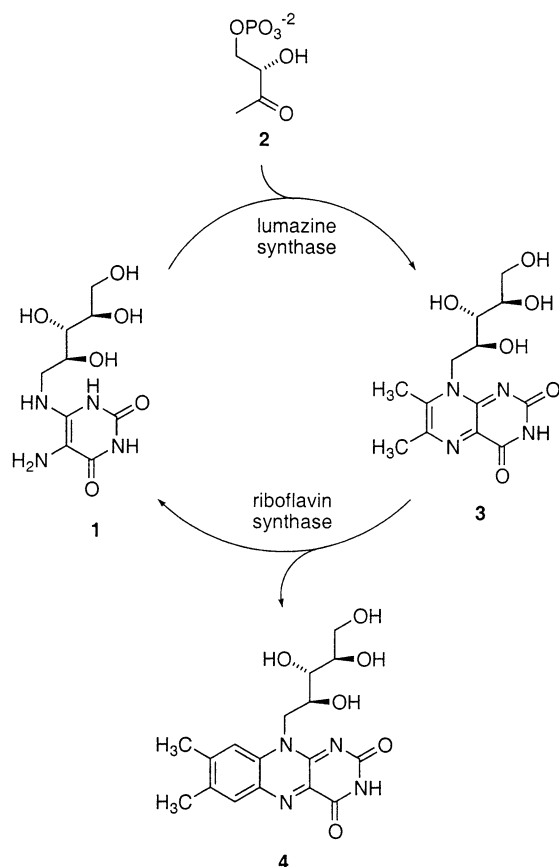
(10) Trach, V. M.; Logvinenko, E. M.; Schlee, D.; Reinbothe, H.; Shavlovsky *Biochem. Physiol. Pflanzen.* **1982**, *177*, 585–592.

(11) Sibirnyi, A. A.; Shavlovskii, G. M.; Ksheminskaya, G. P.; Orlovskaya, A. G. *Mikrobiologiya* **1976**, *46*, 376–378.

(12) Sibirnyi, A. A.; Shavlovskii, G. M.; Ksheminskaya, G. P.; Orlovskaya, A. G. *Biokhimiya* **1977**, *42*, 1841–1851.

(13) Perl, M.; Kearny, E. B.; Singer, T. P. In *Flavins and Flavoproteins*; Singer, T. P., Ed.; Elsevier: Amsterdam, 1976; pp 754–761.

SCHEME 1



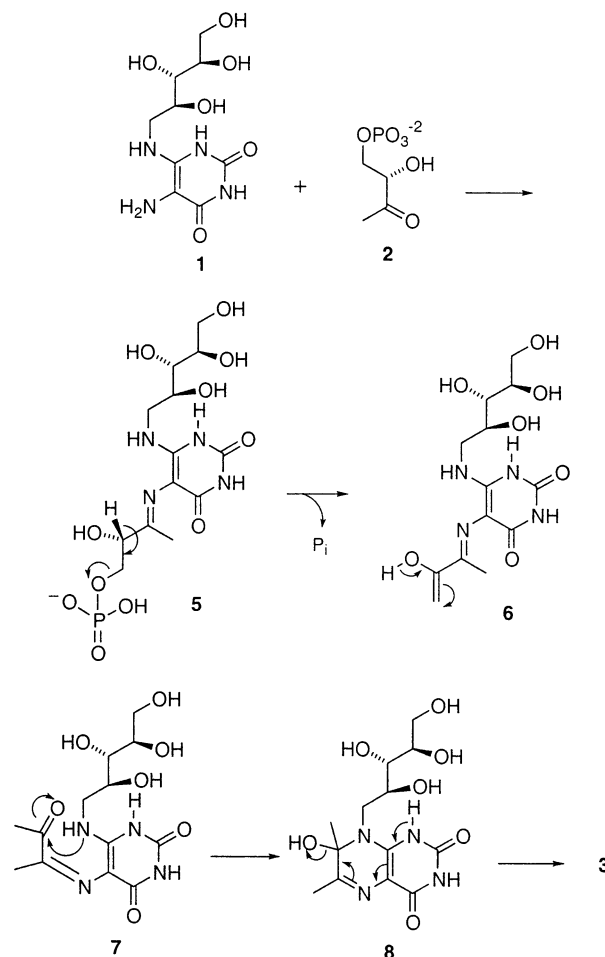
lamino-2,4(1*H*,3*H*)-pyrimidinedione **9** and inorganic phosphate bound to reconstituted, icosahedral, β_{60} *Bacillus subtilis* lumazine synthase capsid.¹⁴ Overlapping the structures of the hypothetical intermediate **5** with the position of enzyme-bound structures of 5-nitro-6-D-ribitylamino-uracil (**9**) and inorganic phosphate as determined by X-ray crystallography makes it evident that the conformation of the phosphate-containing side chain resembles that in structure **5**.¹⁴ This hypothesis is also supported by the crystal structure of the phosphonate **11** bound to *Saccharomyces cerevisiae* lumazine synthase.^{15,16} In the structure of the proposed enzyme-bound hypothetical reaction intermediate **5**, the end of the phosphate-containing side chain is distant from the nucleophilic ribitylamino group, implying that the enol group of **6** would also be initially generated away from the nucleophilic amine. The imine geometry in **5** is unknown. Both (*E*)- and (*Z*)-imines can be modeled into the active site of lumazine synthase with the phosphate and pyrimidine ring occupying approximately the same space as the inorganic phosphate and the pyrimidine ring present in the crystal structure of bound **9**. However, a (*Z*)-imine is required in **7** in order for cyclization to occur. Since the phosphate group of **5** is distant from the amino group, an extensive conformational reorganization of the side chain is required after phosphate elimination in order

(14) Ritsert, K.; Huber, R.; Turk, D.; Ladenstein, R.; Schmidt-Bäse, K.; Bacher, A. *J. Mol. Biol.* **1995**, *253*, 151–167.

(15) Cushman, M.; Mihalic, J. T.; Kis, K.; Bacher, A. *J. Org. Chem.* **1999**, *64*, 3838–3845.

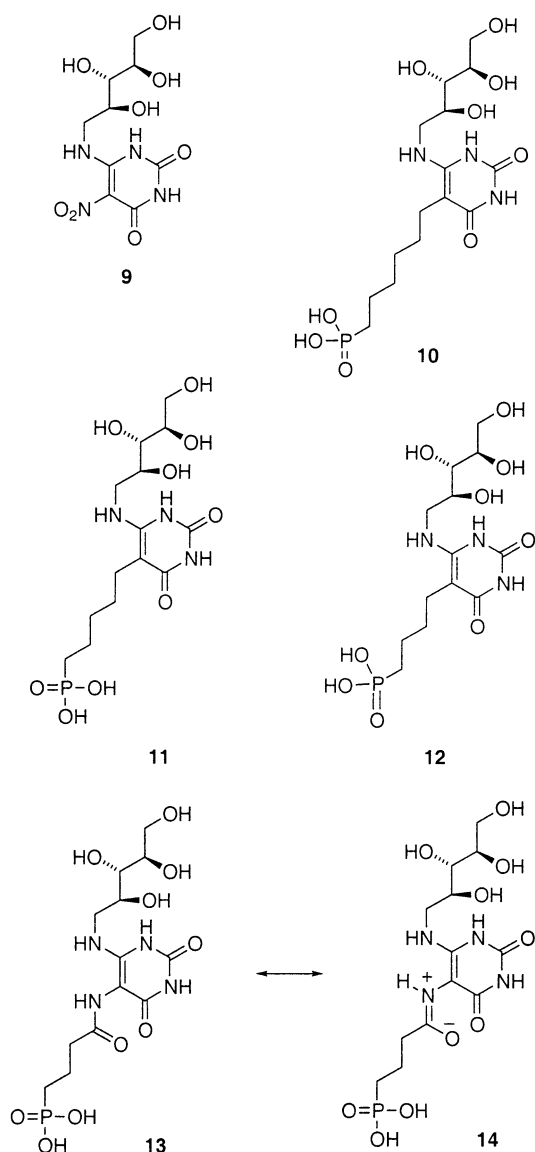
(16) Meining, W.; Mörtl, S.; Fischer, M.; Cushman, M.; Bacher, A.; Ladenstein, R. *J. Mol. Biol.* **2000**, *299*, 181–197.

SCHEME 2



for the ketone of **7** to be brought into close proximity with the secondary amino group so cyclization can occur.

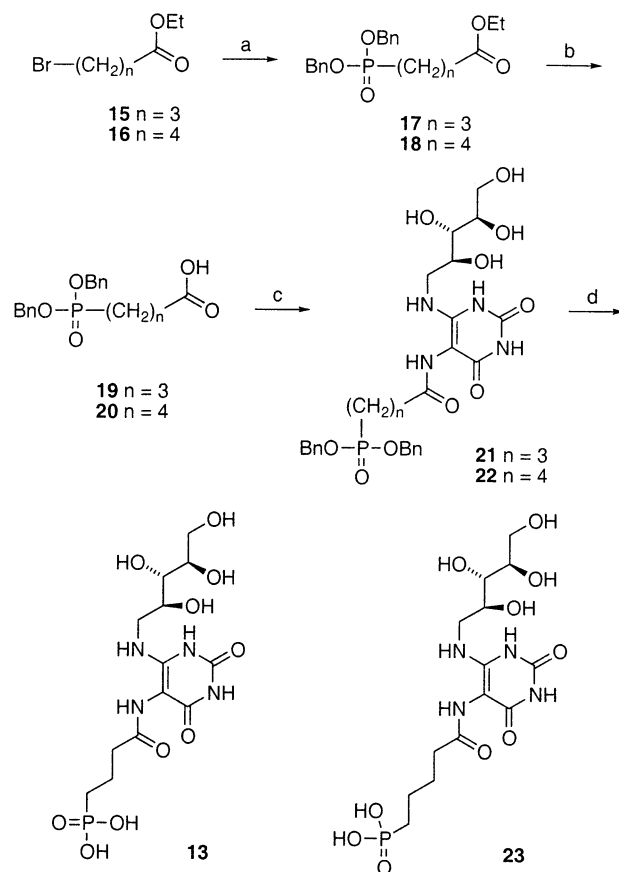
The phosphonate **10**, as well as its lower homologues **11** and **12**, were synthesized and found to be lumazine synthase inhibitors.¹⁵ Their K_i values vs recombinant *B. subtilis* capsids were 130, 180, and 440 μM , respectively. A logical way to increase the potencies of these metabolically stable inhibitors would be to replace the polymethylene chain connecting the phosphonate to the pyrimidine with one that would more closely resemble the hypothetical intermediate **5**. This led us to consider various imine replacements. One possibility would be to replace the imino group of **5** with an amide moiety, and an analogue of **11** containing such a substitution would be compound **13**. The closer resemblance of the amide **13** (vs **11**) to **5** is underlined by the amide resonance form shown in structure **14**, which is often invoked to explain the hindered rotation around amide bonds. In this scenario, the amide oxygen in **13** \leftrightarrow **14** would resemble the methyl group attached to the imino carbon of **5**. On the other hand, if the proposed lumazine synthase inhibitor **13** and related compounds were inactive, it would still be an interesting result that might possibly shed some light on the structural requirements for binding to the active site of lumazine synthase. Therefore, we decided to synthesize **13** and several analogues and test them as inhibitors of *Bacillus subtilis* lumazine synthase and *Escherichia coli* riboflavin synthase.



Results and Discussion

The syntheses of the desired phosphonate **13** and its higher homologue **23** are outlined in Scheme 3. Deprotonation of dibenzyl phosphite with sodium hydride in DMF afforded the corresponding anion, which upon reaction with commercially available ethyl 4-bromobutyrate (**15**) and ethyl 5-bromovalerate (**16**) provided the expected phosphonates **17** and **18**, respectively. Hydrolysis of the esters **17** and **18** was accomplished with lithium hydroxide in aqueous THF to provide the carboxylic acids **19** and **20**, respectively. Treatment of the carboxylic acids **19** and **20** with oxalyl chloride in methylene chloride yielded the corresponding acid chlorides, which were then reacted with 5-amino-6-D-ribitylamino-uracil, prepared by catalytic reduction of the nitro compound **9**,¹⁷ to produce the desired amides **21** and **22**, respectively. Debzilylation was then accomplished by catalytic hydrogenolysis over palladium on carbon, resulting in the deprotected phosphonates **13** and **23**.

SCHEME 3^a

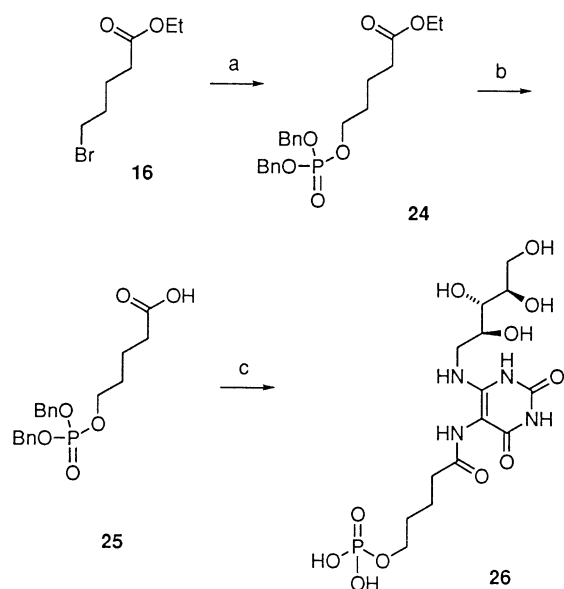


^a Reagents: (a) $(\text{BnO})_2\text{P}(\text{O})\text{H}$, NaH, DMF or THF, **28** and 51%; (b) LiOH aqueous THF, 81%; (c) (i) $(\text{COCl})_2$, CH_2Cl_2 , (ii) NEt_3 , aqueous CH_3CN , 5-amino-6-ribitylamino-uracil; (d) H_2 , Pd/C, 85%.

The synthesis of a phosphate analogue **26** of the phosphonate **23** is shown in Scheme 4. Reaction of ethyl 5-bromovalerate (**16**) with silver dibenzyl phosphite in toluene afforded the expected phosphonate **24**. Hydrolysis of the ethyl ester group of **24** was accomplished with lithium hydroxide in THF. Conversion of the acid **25** to its acid chloride, reaction of the acid chloride with the primary amino group of 5-amino-6-D-ribitylamino-uracil, and catalytic hydrogenolysis of the two benzyl protecting groups afforded the phosphate **26**.

The hypothetical reaction intermediate analogues **13**, **23**, and **26** were tested as inhibitors of recombinant *B. subtilis* lumazine synthase capsids and *E. coli* riboflavin synthase. The results of these enzyme inhibition studies are listed in Table 1. For comparison, the enzyme inhibition data for the previously reported phosphonates **10**, **11**, and **12** are also reported in Table 1. The enzyme kinetics plots are displayed in Figures 1 and 2. Contrary to expectation, the new amides **13**, **23**, and **26** had either no observable activity or very low activity vs lumazine synthase. All of them were less active than the phosphonates **10**, **11**, and **12**. The most active of the series, compound **26**, displayed a K_i of 830 μM , vs 130 μM for the phosphonate **10**. The reasons for the low activity of the amides are not clear, since they can be docked readily in the active site of lumazine synthase by molecular modeling (data not shown).

(17) Kis, K.; Kugelbrey, K.; Bacher, A. *J. Org. Chem.* **2001**, *66*, 2555–1559.

SCHEME 4^a

^a Reagents: (a) AgOP(O)(OBn)₂, toluene, 95%; (b) LiOH, aqueous THF, 81%; (c) (i) (COCl)₂, CH₂Cl₂, (ii) 5-amino-6-D-ribitylamouracil, (iii) H₂, Pd(OH)₂/C, 40%.

TABLE 1. Inhibition Constants vs Lumazine Synthase and Riboflavin Synthase

compd	lumazine synthase ^a K_i (μ M)	riboflavin synthase ^b K_i (μ M)
10	130 \pm 33 (K_i , mixed inhibition)	>1000
	140 \pm 15 (K_{is})	
11	180 \pm 88 (K_i , mixed inhibition)	>1000
	350 \pm 22 (K_{is})	
12	440 \pm 200 (K_i , mixed inhibition)	>1000
	640 \pm 300 (K_{is})	
13	>860 ^c	160 \pm 87 (mixed inhibition) 7.7 \pm 2.3 (K_s) 390 \pm 63 (K_{is})
23	>1000	170 \pm 79 (mixed inhibition) 6.8 \pm 2 (K_s) 590 \pm 90 (K_{is})
		190 \pm 39 (mixed inhibition)
		8200 \pm 3100 (K_{is})
		5.7 \pm 0.9 (K_s)
26	830 \pm 170 (mixed inhibition)	
	2000 \pm 360 (K_{is})	
	33 \pm 3.2 (K_s)	

^a Recombinant β_{60} capsids from *B. subtilis*. ^b Recombinant riboflavin synthase from *E. coli*. ^c K_{is} is the equilibrium constant for the reaction EI + S \rightleftharpoons EIS. There was 55% enzyme activity remaining at an inhibitor concentration of 860 μ M.

The phosphate **26** is close in structure to the phosphonate **23**. At a concentration of 860 μ M of the phosphonate **23**, there is still 55% of the initial lumazine synthase enzyme activity remaining. The K_i of **26** is 830 μ M, indicating that the replacement of the phosphonate by a phosphate group resulted in a slight increase in enzyme inhibitory activity. This seems reasonable because the hypothetical intermediate **5** is a phosphate. At the physiological pH of 7.4, phosphonates are mainly monoanionic, whereas phosphates are dianionic. More specifically, the pK_{as} of methyl phosphate, CH₃OPO(OH)₂, are 1.6 and 6.3, while the corresponding values of methyl phosphonate, CH₃PO(OH)₂, are 2.3 and 7.7.¹⁸ It can therefore be expected that the electronic charge of the

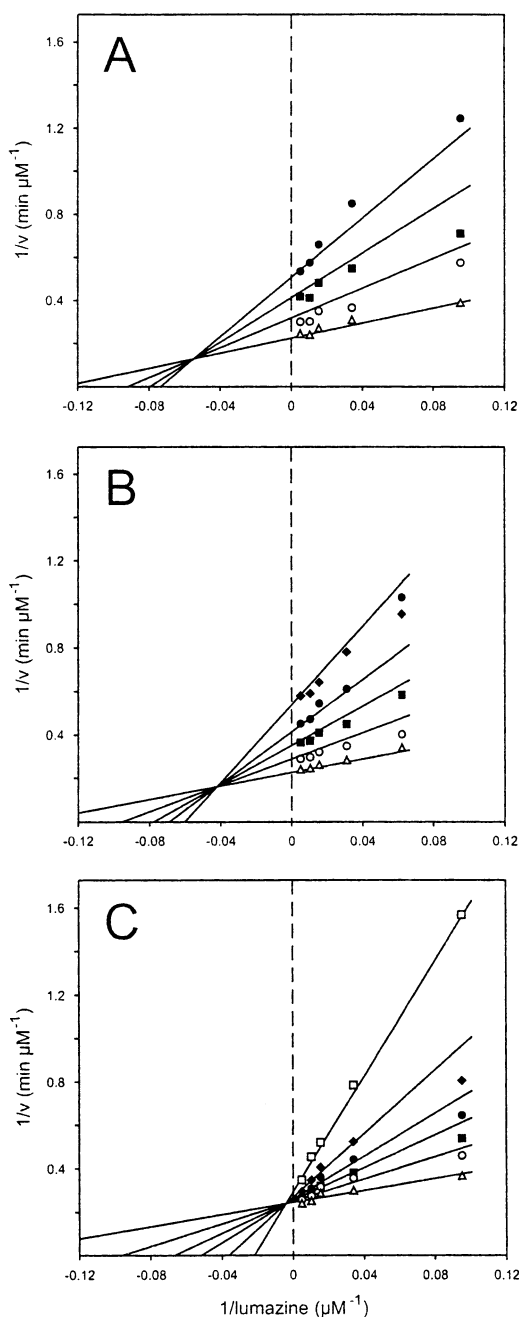


FIGURE 1. Lineweaver–Burk plots of the inhibition of riboflavin synthase by: (A) **13**, (B) **23**, and (C) **26**. Concentrations of the substrate in the experiments portrayed in graphics A and C varied between 11 and 200 μ M, while for those for B, it ranged from 16 to 200 μ M. Inhibitor concentrations: \square , 1613 μ M; \blacklozenge , 808 μ M; \bullet , 484 μ M; \blacksquare , 323 μ M; \circ , 161 μ M; \triangle , 0 μ M. Initial velocities of riboflavin formation, v , were determined at steady-state conditions with varying amounts of substrate, s , and inhibitor. The kinetic data were fitted with a nonlinear regression method using the program DynaFit from P. Kuzmich (1996). Different kinetic models were considered, and the most likely inhibition mechanism was determined to be mixed-type inhibition for all three compounds.

phosphate of **26** would more closely resemble the charge of the phosphate of natural substrate **5** than the phosphonate of **23** would.

Even more surprising than the low activity displayed by the amides vs lumazine synthase was their relatively

(18) Kabachnik, M. I.; Mastrukova, T. A.; Shipov, A. E.; Melentyeva, T. A. *Tetrahedron* **1960**, *9*, 10–28.

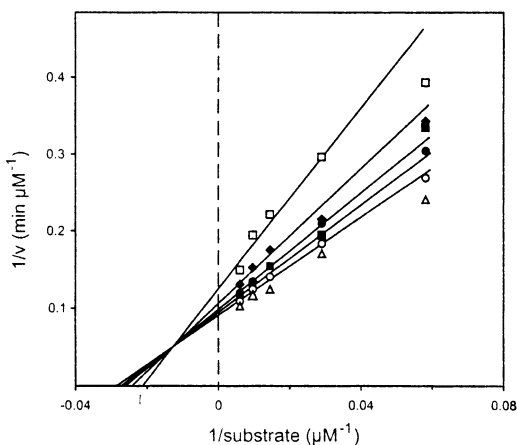
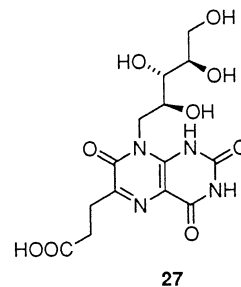


FIGURE 2. Lineweaver–Burk plot of the inhibition of lumazine synthase by **26**. The substrate concentration was 170 μM . Inhibitor concentrations: \square , 882 μM ; \blacklozenge , 431 μM ; \bullet , 259; \blacksquare , 172 μM ; \circ , 86 μM ; \triangle , 0 μM . Initial velocities of riboflavin formation, v , were determined at steady-state conditions with varying amounts of substrate, s , and inhibitor. The kinetic data were fitted with a nonlinear regression method using the program DynaFit from P. Kuzmic (1996). Different kinetic models were considered, and the most likely inhibition mechanism was determined to be mixed-type inhibition.

good activity as riboflavin synthase inhibitors. Compounds **13**, **23**, and **26** displayed K_i values of 160, 170, and 190 μM , respectively, as inhibitors of *E. coli* riboflavin synthase (Table 1). The K_m of the substrate **3** vs *E. coli* riboflavin synthase is 16 μM .¹⁹ The activity of **13**, **23**, and **26** as riboflavin synthase inhibitors was totally unexpected because the previously reported phosphonates **10**, **11**, and **12** were all completely inactive when tested as riboflavin synthase inhibitors.¹⁵ Consequently, it seems that the introduction of an amide into the chain linking the phosphonate to the uracil ring has resulted in an astounding reversal in selectivity for riboflavin synthase vs lumazine synthase inhibition. An X-ray structure of *E. coli* riboflavin synthase, which contains three identical subunits, has been published along with a hypothetical model of bound 6,7-dimethyl-8-D-ribityl-lumazine (**3**).²⁰ According to the model, as well as NMR studies of the structure of the N-terminal domain of riboflavin synthase,²¹ the active site of the enzyme is derived from the intermolecular juxtaposition of residues belonging to both of the barrels in the C-terminal and N-terminal domains of two monomer units, with one substrate molecule bound to each barrel. A model was constructed for the binding of two molecules of inhibitor **13** to *E. coli* riboflavin synthase by manually positioning its structure as suggested by the published model.²⁰ The initial orientations of the ligand molecules in the active site were also consistent with the X-ray structure of monomeric *Schizosaccharomyces pombe* riboflavin syn-

thase complexed with 6-carboxyethyl-7-oxo-8-D-ribityl-lumazine (**27**).²²



Energy minimization then led to the structure of the enzyme–inhibitor complex displayed in Figure 3. The N-barrel residues in Figure 3 are colored orange, while the C-barrel residues are green. The inhibitor **13** bound to the N-barrel is colored magenta, while the inhibitor **13** bound in the C-barrel is white. The water molecules in Figure 3 are red and blue. The structure of the complex in Figure 3 shows quite clearly that the active site of *E. coli* riboflavin synthase can accommodate two molecules of the inhibitor with the pyrimidine rings stacked and the ribitylamino groups pointing in opposite directions. This orientation of the ribityl chains is consistent with the known regiochemistry of the enzyme-catalyzed reaction, which indicates that the ribityl chains of the substrate **3** are also projected outward from the ring in opposite directions.³ The aliphatic portions of the phosphonate chains also appear to be oriented in a parallel fashion that would allow for van der Waals and hydrophobic attractions. Multiple hydrogen bonding interactions are apparent between the ligand molecules and the surrounding water and the protein side chains.

Experimental Section

General. Melting points were determined in capillary tubes on a Mel-Temp apparatus and are uncorrected. The proton nuclear magnetic resonance spectra (¹H NMR) were determined at 300 MHz. Microanalyses were performed at the Purdue Microanalysis Laboratory, and all values were within 0.4% of the calculated compositions. Silica gel (230–400 mesh) was used for column chromatography.

Ethyl 4-(Dibenzylphosphono)butyrate (17). Under an atmosphere of argon, dibenzyl phosphite (1.83 g, 6.99 mmol) was added to a suspension of sodium hydride (0.168 g, 6.99 mmol) in anhydrous THF at 60 °C. After hydrogen liberation ceased (30 min), ethyl 4-bromobutyrate (**15**) (1 mL, 6.99 mmol) was then added dropwise, and the mixture was heated to reflux overnight. THF was then removed using reduced pressure, and the oily residue was dissolved in ether (15 mL), washed with water, brine, and dried over sodium sulfate. After the ether was removed, the oil was purified by flash chromatography (3 × 40 cm column of SiO₂, 230–400 mesh) eluting with 1:1 hexane–ethyl acetate to give **17** (0.727 g, 28%) as a light yellow oil: IR (film) 1731, 1498, 1455, 1378, 1243, 995 cm⁻¹; ¹H NMR (CDCl₃, 300 MHz) δ 7.32 (s, 10 H), 4.90–5.11 (m, 4 H), 4.07 (q, $J = 7.1$ Hz, 2 H), 2.33 (t, $J = 6.7$ Hz, 2 H), 1.73–1.93 (m, 4 H), 1.21 (t, $J = 7.1$ Hz, 3 H); ¹³C NMR (CDCl₃) δ 172.6, 136.4, 128.6, 128.4, 127.9, 67.1, 60.4, 34.3, 25.3, 18.0, 14.2; EIMS m/z 377 (100, MH⁺). Anal. Calcd for C₂₀H₂₅O₅P: C, 63.82; H, 6.69. Found C, 64.05; H, 6.69.

(22) Gerhardt, S.; Schott, A.-K.; Fischer, M.; Kairies, N.; Cushman, M.; Illarionov, B.; Eisenreich, W.; Bacher, A.; Huber, R.; Steinbacher, S. *Structure* **2002**, unpublished results.

(19) Bacher, A.; Eberhardt, S.; Fischer, M.; Mörtl, S.; Kis, K.; Kugelbrey, K.; Scheuring, J.; Schott, K. In *Methods in Enzymology*; McCormick, D. B., Suttie, J. W., Wagner, C., Eds.; Academic Press: San Diego, 1997; Vol. 280, pp 389–399.

(20) Liao, D.-I.; Wawrzak, Z.; Calabrese, J. C.; Viitanen, P. V.; Jordan, D. B. *Structure* **2001**, *9*, 399–408.

(21) Truffault, V.; Coles, M.; Diericks, T.; Abelmann, K.; Eberhardt, S.; Lüttgen, H.; Bacher, A.; Kessler, H. *J. Mol. Biol.* **2001**, *309*, 949–960.

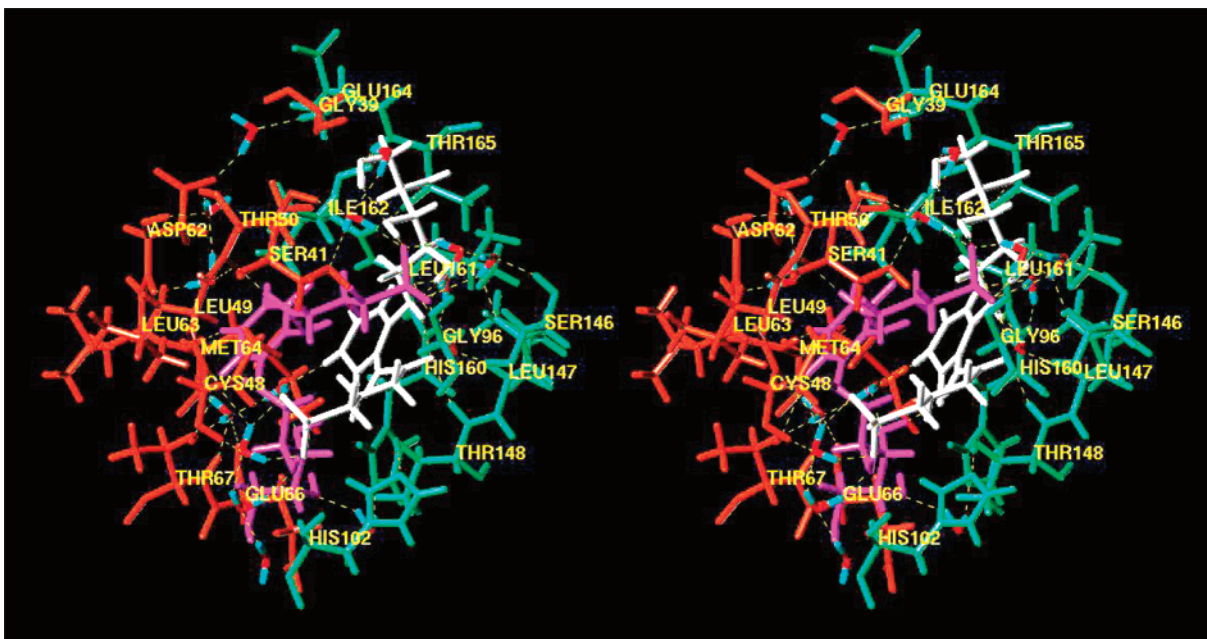


FIGURE 3. Hypothetical model for the binding of two molecules of inhibitor **13** in the active site in *E. coli* riboflavin synthase. Magenta, compound **13** bound to the N-barrel; white, compound **13** bound to the C-barrel; orange, N-barrel residues; green, C-barrel residues; red and blue, water molecules. The structure is programmed for wall-eyed viewing.

Ethyl 5-(Dibenzylphosphono)valerate (18). To a stirred suspension of NaH (0.6 g, 0.025 mol) in dry DMF (30 mL) under argon atmosphere was added dibenzyl phosphite (5.25 g, 0.02 mol) at room temperature. After 15 min of stirring, ethyl 5-bromovalerate (**16**) (4.18 g, 0.02 mol) was added, and the entire mixture was stirred at room temperature for 24 h. DMF was then removed using reduced pressure. The resulting oil was taken into diethyl ether (60 mL), washed with water and brine, and dried over sodium sulfate. The ether solution was then concentrated, and the remaining oil was purified using silica gel column chromatography eluting with ethyl acetate–hexane (from 5:1 to 2:1). Pure product **18** (4.0 g, 51%) was obtained as a light yellow oil: IR (film) 2958, 1732, 1456, 1374, 1251, 996 cm^{-1} ; $^1\text{H NMR}$ (300 MHz, CDCl_3) δ 7.34 (s, 10 H), 4.91–5.12 (m, 4 H), 4.10 (q, $J = 7$ Hz, 2 H), 2.23 (t, $J = 7$ Hz, 2 H), 1.61–1.79 (m, 6 H), 1.21 (t, $J = 7$ Hz, 3 H); HREIMS (M^+) calcd for $\text{C}_{21}\text{H}_{27}\text{O}_5\text{P}$ m/z 390.1596, found 390.1599. Anal. Calcd for $\text{C}_{21}\text{H}_{27}\text{O}_5\text{P}$: C, 64.61; H, 6.97; P, 7.93. Found: C, 64.71; H, 7.25; P, 7.68.

4-(Dibenzylphosphono)butyric Acid (19). Lithium hydroxide monohydrate (0.017 g, 0.4 mmol) and ethyl 4-(dibenzylphosphono)butyrate (**17**) (0.1 g, 0.3 mmol) were stirred in a THF–water solution (1:1, 6 mL) at room temperature for 1 h. THF was then removed with reduced pressure, and the resulting water solution was washed with ether (2×10 mL) and then acidified with concentrated HCl. The product was extracted out of the acidic solution with ether (3×10 mL), and the solution was washed with brine, dried over sodium sulfate, and rotary evaporated to give **19** (0.075 g, 81%) as a clear oil: IR (film) 2954, 1727, 1498, 1456, 1407 1215, 998 cm^{-1} ; $^1\text{H NMR}$ (CDCl_3 , 300 MHz) δ 7.32 (s, 10 H), 4.90–5.07 (m, 4 H), 2.39 (t, $J = 6.8$ Hz, 2 H), 1.77–1.96 (m, 4 H); $^{13}\text{C NMR}$ (CDCl_3) δ 176.5, 136.1, 128.6, 128.4, 127.9, 67.3, 34.0, 25.0, 17.7; HREIMS (M^+) calcd for $\text{C}_{18}\text{H}_{21}\text{O}_5\text{P}$ m/z 348.1127, found 348.1122. Anal. Calcd for $\text{C}_{18}\text{H}_{21}\text{O}_5\text{P}$: C, 62.07; H, 6.08. Found: C, 61.73; H, 6.16.

5-(Dibenzylphosphono)valeric Acid (20). Ethyl 5-(dibenzylphosphono)valerate (**18**) (0.55 g, 1.41 mmol) and lithium hydroxide (0.81 g, 1.93 mmol) were stirred in a 1:1 THF–water solution (15 mL) for 2 h. THF was then removed using reduced pressure, and the remaining aqueous solution was acidified with concentrated HCl and extracted with ether (2×20 mL).

The ether layer was washed with brine (20 mL), dried over sodium sulfate, and concentrated to give a clear oil (0.41 g, 81%): $^1\text{H NMR}$ (300 MHz, CDCl_3) δ 7.33 (s, 10 H), 4.91–5.07 (m, 4 H), 2.29 (t, $J = 7$ Hz, 2 H), 1.64–1.81 (m, 6 H); CIMS (MH^+) m/z 363. Anal. Calcd for $\text{C}_{19}\text{H}_{23}\text{O}_5\text{P}$: C, 62.98; H, 6.40; P, 8.55. Found: C, 63.12; H, 6.42; P, 8.37.

5-(4-Dibenzylphosphonobutyl)amino-6-D-ribitylamino-uracil (21). 4-(Dibenzylphosphono)butyric acid (**19**) (0.5 g, 1.4 mmol) was dissolved in dichloromethane (20 mL) and a solution of oxalyl chloride in dichloromethane (2 M, 1 mL), and two drops of DMF were added. After being stirred at room temperature for an additional 2 h, the reaction mixture was evaporated and then coevaporated twice with dichloromethane (20 mL) to remove traces of oxalyl chloride. The residue was dissolved in dry acetonitrile (10 mL) and added to a solution of 5-amino-6-D-ribityluracil, freshly prepared from 5-nitro-6-D-ribityluracil (**9**) (0.5 g, 1.6 mmol),^{17,23,24} and triethylamine (2 mL) in water (20 mL). The mixture was stirred at room temperature for 12 h and then evaporated to dryness. The residue was washed by acetonitrile and then purified by chromatography on a silica gel column (*i*-PrOH– H_2O , from 1:20 to 1:6) to afford **21** (0.5 g, 58%) as an amorphous, hygroscopic solid: $^1\text{H NMR}$ (300 Hz, D_2O) δ 7.35 (m, 10 H), 5.1–4.9 (m, 4 H), 3.92 (m, 1 H), 3.80 (m, 1 H), 3.68 (m, 2 H), 3.59–3.45 (m, 3 H), 2.45 (t, $J = 7.2$ Hz, 2 H), 2.1–1.9 (m, 4 H); PDMS m/z 607 (MH^+); $^{13}\text{C NMR}$ (MeOH) δ 176.5, 163.6, 155.0, 152.3, 137.7, 129.7, 129.5, 129.1, 88.1, 74.4, 73.8, 73.2, 68.7, 54.5, 46.1, 36.6, 36.3, 26.4, 24.5, 19.3; PDMS m/z 607 (MH^+). Anal. Calcd for $\text{C}_{27}\text{H}_{35}\text{N}_4\text{O}_{10}\text{P} \cdot 2.3 \text{H}_2\text{O}$: C, 50.05; H, 6.16. Found: C, 50.02; H, 6.04.

5-(4-Phosphonobutyl)amino-6-D-ribitylamino-uracil (13). A mixture of compound **21** (0.5 g, 0.82 mmol) and $\text{Pd}(\text{OH})_2$ on charcoal (0.1 g, 20%) in 1:1 MeOH–water (1:1) was hydrogenated under an H_2 atmosphere for 12 h. The catalyst was removed by filtration, and the filtrate was concentrated to dryness. The residue was applied to an anion-exchange resin column (Dowex 1 \times 2–400) eluted with distilled

(23) Cresswell, R. M.; Wood, H. S. C. *J. Chem. Soc.* **1960**, 4768–4775.

(24) Cushman, M.; Yang, D.; Kis, K.; Bacher, A. *J. Org. Chem.* **2001**, *66*, 8320–8327.

water and 10% HCOOH. After concentration of the pooled fractions, the residue was treated with methanol to afford a white precipitate **13** (0.3 g, 85%) as an amorphous solid: ^1H NMR (300 Hz, D_2O) δ 3.82 (m, 1 H), 3.70 (m, 2 H), 3.59–3.45 (m, 3 H), 3.39 (m, 1 H), 2.40 (t, $J = 7.3$ Hz, 2 H), 1.7–1.9 (m, 2 H), 1.65–1.5 (m, 2 H). PDMS m/z 427 (MH^+). Anal. Calcd for $\text{C}_{13}\text{H}_{23}\text{N}_8\text{O}_{10}\text{P}(2.0\text{H}_2\text{O} + 0.9\text{HCO}_2\text{H})$: C, 34.54; H, 5.64; N, 10.89. Found C, 34.53; H, 5.47; N, 11.07.

5-(5-Phosphonovaleryl)amino-6-D-ribitylamino-uracil (23). 5-(Dibenzylphosphono)valeric acid (**20**) (1.5 g, 4.1 mmol) was dissolved in dichloromethane (20 mL) and a solution of oxalyl chloride in dichloromethane (2M, 2 mL), and two drops of DMF were added. After being stirred at room temperature for an additional 2 h, the reaction mixture was evaporated and then coevaporated twice with dichloromethane (20 mL) to remove traces of oxalyl chloride. The residue was dissolved in dry acetonitrile (10 mL) and added to a solution of 5-amino-6-D-ribityluracil hydrochloride^{17,23,24} (0.5 g, 1.5 mmol) and triethylamine (2 mL) in water (20 mL). The mixture was stirred at room temperature for 12 h and then evaporated to dryness. The residue was washed with acetonitrile to give **22** (0.7 g, 75%) as a hygroscopic solid that was used without further purification. A mixture of compound **22** (0.5 g, 0.8 mmol) and $\text{Pd}(\text{OH})_2$ on charcoal (0.1 g, 20%) in 1:1 MeOH–water (20 mL) was hydrogenated under an H_2 atmosphere for 12 h. The catalyst was removed by filtration, and the filtrate was concentrated to dryness. The residue was treated with methanol to afford an amorphous white precipitate **23** (0.3 g, 85%): ^1H NMR (300 Hz, D_2O) δ 3.81 (m, 1 H), 3.68 (m, 2 H), 3.59–3.45 (m, 3 H), 3.39 (m, 1 H), 2.35 (t, $J = 7.2$ Hz, 2 H), 1.63–1.48 (m, 6 H). Anal. Calcd for $\text{C}_{14}\text{H}_{25}\text{N}_8\text{O}_{10}\text{P}\cdot 2.1\text{H}_2\text{O}$: C, 35.17; H, 6.16; N, 11.72. Found C, 35.08; H, 5.90; N, 11.48.

Ethyl 5-(Dibenzylphosphonoxy)valerate (24). A mixture of ethyl 5-bromovalerate (**16**) (0.87 g, 4.15 mmol) and silver dibenzyl phosphate (1.6 g, 4.15 mmol) in toluene (50 mL) was heated at reflux for 5 h under N_2 . After the mixture was cooled, the precipitate was removed by filtration and the filtrate was concentrated to give **24** (1.6 g, 95%) as a colorless oil: ^1H NMR (300 Hz, CDCl_3) δ 7.35 (m, 10 H), 5.05–5.00 (m, 4 H), 4.14 (q, $J = 7.1$ Hz, 2 H), 4.02 (m, 2 H), 2.29 (m, 2 H), 1.64 (m, 4 H), 1.26 (t, $J = 7.1$ Hz, 3 H); ^{13}C NMR (CDCl_3) δ 173.1, 135.8, 128.5, 127.8, 69.1, 67.2, 60.2, 33.5, 29.4, 20.8, 14.1; EIMS m/z 429 (100, MNa^+). Anal. Calcd for $\text{C}_{21}\text{H}_{27}\text{O}_6\text{P}$: C, 62.06; H, 6.70. Found C, 62.00; H, 6.79.

5-(Dibenzylphosphonoxy)valeric Acid (25). Ethyl 5-(dibenzylphosphono)valerate **24** (1.5 g, 3.6 mmol) and lithium hydroxide (0.2 g, 8 mmol) were mixed in 1:1 THF–water (25 mL) for 5 h. THF was then removed under reduced pressure, and the remaining aqueous solution was acidified with concentrated HCl and extracted with diethyl ether (3 \times 50 mL). The ether layer was washed with brine, dried over sodium sulfate, and concentrated in vacuo. The residue was purified by silica gel column chromatography (1:2:0.1 hexane–AcOEt–AcOH) to afford **25** (1.1 g, 81%) as a colorless oil: ^1H NMR (300 Hz, CDCl_3) δ 7.37 (m, 10 H), 5.10–4.98 (m, 4 H), 4.02 (m, 2 H), 2.34 (m, 2 H), 1.67 (m, 4 H); ^{13}C NMR (CDCl_3) δ 177.9, 135.7, 128.5, 127.9, 69.3, 67.3, 33.2, 29.4, 20.6; EIMS m/z 379 (100, MH^+). Anal. Calcd for $\text{C}_{19}\text{H}_{23}\text{O}_6\text{P}$: C, 60.32; H, 6.13. Found C, 60.45; H, 6.22.

5-(5-Phosphonoxyvaleryl)amino-6-D-ribitylamino-uracil (26). 5-(Dibenzylphosphonoxy)valeric acid (**25**) (1.0 g, 2.6 mmol) was dissolved in dichloromethane (20 mL) at 0 $^\circ\text{C}$ and a solution of oxalyl chloride in dichloromethane (2M, 2 mL), and two drops of DMF were added. After being removed from the cooling bath and stirred at room temperature for an additional 2 h, the reaction mixture was evaporated and then coevaporated twice with dichloromethane (20 mL) to provide the acid chloride as a colorless oil: ^1H NMR (300 Hz, CDCl_3) δ 7.37 (m, 10 H), 5.10–4.98 (m, 4 H), 3.98 (q, $J = 6$ Hz, 2 H), 2.82 (t, $J = 6$ Hz, 2 H), 1.65 (m, 4 H). The acid chloride was dissolved in dry acetonitrile (10 mL) and added dropwise to a solution of 5-amino-6-D-ribitylamino-uracil,^{17,23,24} freshly prepared by catalytic reduction of 5-nitro-6-D-ribitylamino-uracil

(**9**) (0.5 g, 1.6 mmol) and triethylamine (2 mL) in water (20 mL). The mixture was stirred at room temperature for 12 h and then evaporated to dryness. The residue was then dissolved in a mixture of 1:1 MeOH–water (20 mL) and hydrogenated under an H_2 atmosphere in the presence of $\text{Pd}(\text{OH})_2$ on charcoal (0.1 g, 20%) for 12 h. The catalyst was removed by filtration, and the filtrate was concentrated to dryness. The residue was basified with a few drops of triethylamine and then applied on an anion-exchange resin column (Dowex 1 \times 2–400), eluted with distilled water and 10% HCOOH. After concentration of pooled fractions, the residue was treated with ethanol to precipitate **26** (0.29 g, 40%) as an amorphous solid: ^1H NMR (300 Hz, D_2O) δ 3.86 (m, 3 H), 3.68 (m, 2 H), 3.58–3.45 (m, 3 H), 3.39 (m, 1 H), 2.38 (m, 2 H), 1.62 (m, 4 H); ESMS m/z 457 (MH^+). Anal. Calcd for $\text{C}_{14}\text{H}_{25}\text{N}_4\text{O}_{11}\text{P}\cdot 5.0\text{H}_2\text{O}\cdot 0.7\text{HCOOH}$: C, 35.48; H, 5.55; N, 11.26. Found C, 35.59; H, 5.78; N, 11.03.

Molecular Modeling. Using Sybyl (version 6.5; Tripos, Inc., 1998), we downloaded the X-ray crystal structure of *E. coli* riboflavin synthase (1I8D), and two molecules of the ligand **13** were docked and oriented as suggested by the published model of the binding of two molecules of the substrate **3** in the active site.²⁰ The C- and N-terminal groups were changed to neutral carboxylic acid and amino groups, and hydrogens were added to the protein structure and to the oxygens of the water molecules. MMFF94 charges were loaded, and a 6 \AA spherical subset including and surrounding the two ligand molecules was then energy minimized using the Powell method to a termination gradient of 0.05 kcal/mol while employing the MMFF94 force field. The remaining portion of the protein was held rigid using the aggregate function during energy minimization. Figure 3 was constructed by displaying the amino acid residues in the C- and N-barrels surrounding the two ligand molecules. The maximum distance between donor and acceptor atoms contributing to the hydrogen bonds shown in Figure 3 was set to 2.8 \AA .

Lumazine Synthase Assay.²⁵ Reaction mixtures contained 100 mM potassium phosphate, pH 7.0, 5 mM EDTA, 5 mM dithiothreitol, inhibitor (0–86 μM), 170 μM 5-amino-6-ribitylamino-2,4(1*H*,3*H*)-pyrimidinedione (**1**), and lumazine synthase (30 μg , specific activity 12.5 $\mu\text{mol mg}^{-1}\text{h}^{-1}$) in a total volume of 560 μL . Inhibitor concentrations ranged between 0 and 862 μM . The solution was incubated at 37 $^\circ\text{C}$, and the reaction was started by the addition of a small volume (20 μL) of L-3,4-dihydroxy-2-butanone 4-phosphate to a final concentration of 50–310 μM . The velocity/substrate data were fitted for all inhibitor concentrations with a nonlinear regression method using the program DynaFit.²⁶ Different inhibition models were considered for the calculation. K_i values \pm standard deviations were obtained from the fit under consideration of the most likely inhibition model.

Riboflavin Synthase Assay.²⁷ Reaction mixtures contained buffer (100 mM potassium phosphate, 10 mM EDTA, 10 mM sodium sulfite), inhibitor (0–87 μM), and riboflavin synthase (10 μg , specific activity 50 $\mu\text{mol mg}^{-1}\text{h}^{-1}$). Inhibitor concentrations ranged between 0 and 1.6 mM. After preincubation, the reactions were started by the addition of various amounts of 6,7-dimethyl-8-ribityllumazine (**3**) (20–200 μM) to a total volume of 570 μL . The formation of riboflavin (**4**) was measured online with a computer-controlled photometer at 470 nm ($\epsilon_{\text{riboflavin}} = 9100\text{ M}^{-1}\text{cm}^{-1}$). The K_i evaluation was performed in the manner described above.

Acknowledgment. This research was made possible by NIH Grant GM51469 as well as by support from the Deutsche Forschungsgemeinschaft and Fonds der Chemischen Industrie.

JO020144R

(25) Kis, K.; Bacher, A. *J. Biol. Chem.* **1995**, *270*, 16788–16795.

(26) Kuzmic, P. *Anal. Biochem.* **1996**, *237*, 260–273.

(27) Eberhardt, S.; Richter, G.; Gimbel, W.; Werner, T.; Bacher, A. *Eur. J. Biochem.* **1996**, *242*, 712–718.